Cloud Assimilation in the Era of CloudSat

Graeme Stephens[1], Angela Benedetti[1], Philip Gabriel[1] and Deborah Vane[2]

[1] *Colorado State University, Department of Atmospheric Science*
Ft. Collins, CO 80523
[2] *Jet Propulsion Laboratory, Oak Grove, Pasadena, Ca*

1 Introduction

Clouds are a vital component of the hydrological cycle of the planet providing the essential source of freshwater used by humankind. Clouds also exert a dominant influence on the energy budget of the planet principally through their influence on radiative processes. As such, understanding how well we predict where and when clouds form and how much water is processed by clouds is vital for advancing the prediction of both weather and climate.

Assimilation of cloud and precipitation measurements into models may be viewed as an essential stage in progress toward both advancing such prediction. This paper introduces some of the basic issues confronting assimilation of cloud and precipitation data and does so by framing the discussion around the cloud information expected from the CloudSat experiment.

The paper begins with a brief description of CloudSat identifying the cloud information to be obtained. The philosophy adopted for development of the algorithms is briefly outlined for two reasons. First the algorithm approach emphasizes the flexibility of the method for adding further information derived from other satellite data matched to those data obtained from CloudSat. This is important given the design of the CloudSat experiment which relies on formation flying with EOS Aqua and thus all measurements provided by that satellite could be integrated with the CloudSat measurements. The second reason for the discussion of CloudSat algorithms is that the approach developed parallels the current philosophy developed for assimilation of data in models and therefore bares directly on the problem of data assimilation.

The paper describes an assimilation experiment in section 5 wherein cloud radar data are assimilated into a model of cirrus cloud. This experiment, and results derived from it, provides both a useful framework to begin to consider broader issues of cloud and precipitation data assimilation and attempts to provide a glimpse at the possible impact cloud radar data offer this assimilation problem.

2 The CloudSat experiment - a brief overview

CloudSat is a multi-satellite, multi-sensor experiment (e.g. Stephens et al., 2001) designed to provide key information about clouds and precipitation that cannot be derived from current or planned observing systems. The CloudSat mission is a partnership between NASA/JPL, the Canadian Space Agency, Colorado State University, the US Air Force and the US Department of Energy. CloudSat makes use tight formation flying with other spacecraft forming an observing system constellation providing near-simultaneous measurements from the combination of sensors from the constellation. CloudSat will be launched in 2003

and will fly in formation with EOS-PM (Aqua) as well as with the proposed PICASSO-CENA experiment carrying an aerosol lidar. The payload of Aqua includes CERES, AIRS, AMSR and MODIS. In this way, CloudSat will integrate the radar measurements with Aqua sensor measurements providing a rich source of information for studying clouds and precipitation.

2.1 Mission Science Goals

The science goals of the mission are:

i) Quantitatively evaluate the representation of clouds and cloud processes in global atmospheric circulation models, leading to improvements in both weather forecasting and climate prediction

ii) Quantitatively evaluate the relationship between the vertical profiles of cloud liquid water and ice content and cloud radiative properties, including the radiative heating by clouds.

iii) Evaluate cloud information derived from other research and operational meteorological spacecraft;

iv) Improve our understanding of the indirect effect of aerosols on clouds by investigating the effect of aerosols on cloud formation

2.2 Payload

The primary CloudSat payload consists of a 94-GHz Cloud Profiling Radar (CPR) which is to provide calibrated radar reflectivity, (*e.g.*, radar backscatter power) as a function of distance from the spacecraft. The CPR will provide a nominal minimum detectable reflectivity factor (hereafter MDS) of approximately -28 dBZ, a 70 dB dynamic range, and a calibration accuracy of 1.5 dB. The radar footprint is 1.4 km, and will be averaged over 0.3 seconds to produce an effective footprint of 4 km (along-track) by 1.4 km (cross-track). The normal mode of operation will yield 500-m vertical resolution between the surface and 25 km with a resolution of cloud boundaries at 250m.

2.3 Products

The mission's primary science goal is to furnish data leading to the retrieval of the information summarized in Table 1. There are two types of products summarized in this table. The first set are referred to as standard products to be produced by the Data Processing Center (DPC) of the project. These standard products are deemed to be necessary for addressing the science objectives of the project. The second group of products listed are experimental products are derived (arguably) from less mature algorithms and contribute in less critical although still important ways to the science of the mission. Notable in this list of products is information about precipitation and examples of this product using a CloudSat 94 GHz radar precipitation retrieval scheme is described below. The list of experimental products will continue to expand as other data are included and new retrieval methods are developed prior to launch.

Product	Property	Resolution/accuracy	Comments
1 Cloud profile mask	Threshold above –28 dBZ	500m	Provides all vertical geometric properties
2 Cloud Classification	Match to selected WMO cloud types	NA	Combines radar and imaging information
3 Cloud Ice Water Content	For clouds above optical depth 0.1	500m 30-50%	Mergers radar and optical depth data. Also uses 1&2 above
4 Cloud Liquid water content	For clouds above optical depth 0.1	500m 30-50%	Mergers radar and optical depth data. Also uses 1&2 above
5 Fluxes and heating rate		TOA/surface fluxes: <10 Wm^{-2} instantaneous Heating rate: 500m 1$Kday^{-1}km^{-1}$	Derived
Experimental Product			
6 Precipitation Occurrence	Reflectivity Threshold Approach	500m	
7 Attenuation mask	Based on sigma_0 analyses	TBD	Identifies occurrence of detectable attenuation - linked to 6 above
8 Rainrate (R)	Z-attenuation algorithm	Resolved R< 10 $mmhr^{-1}$ Convective rain > 10 $mmhr^{-1}$	Will use 6 & 7 above as well as other information, notably AMSR radiances.
9 Extinction profile		500m, resolution TBD	Based on Z-extinction relation constrained MODIS based column-wise optical depth
10 Cloud layer Optical Depth		Cloud layer	MODIS+cloudradar combined optical depth algorithm (connected to 9 above) to produce an optical depth alternative to the MOD06 products
11 Particle Size		For upper cloud layer of profile	As for 10.
12 Cirrus Particle size profile	Applicable only to upper most layer of cirrus	500m	Combines lidar and radar

Table 1 A list of the Standard CloudSat data products and a suggested list of experimental products

3 Measurement and Algorithm Approach

The basis for the estimation of cloud physical parameters listed in Table 1 is essentially based on the unique information that can be derived when active measurements (i.e. the cloud radar) are contrasted with passive measurements (available from Aqua). The benefits of combining these different measurement types into a single cloud observing system has been demonstrated over the past 20 years using measurements from both aircraft and ground based lidar, radar and radiometer systems. Following this approach, CloudSat combines

the radar reflectivity data with optical depth information retrieved from reflected sunlight measurements (Austin and Stephens, 2000). This combination provides essentially independent information about cloud liquid water content and droplet size as illustrated in Fig. 1 showing theoretically calculated relationships between vertically integrated radar reflectivity (IZ), cloud optical depth τ, LWP and effective radius r_e portrayed in the form of contours of LWP and r_e for water droplet clouds. The degree of independence of the IZ-τ information is indicated by the degree to which these contours lie in orthogonal directions to one another.

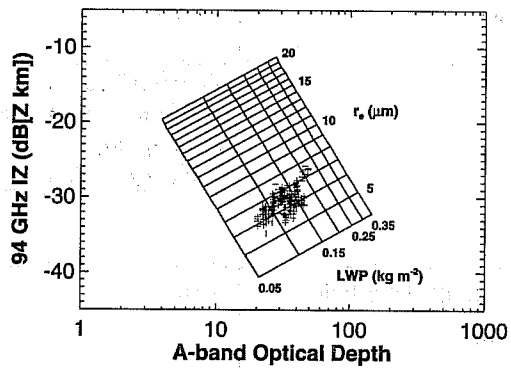

Fig. 1 A theoretically calculated relationship between integrated radar reflectivity IZ and optical depth τ mapped to effective radius and cloud liquid water path. This mapping underscores the degree to which IZ and τ contain essentially independent information about these cloud parameters. The cloud of points on this grid are measurements described in Austin et al. (2001).

3.1 The Algorithm Approach

Figure 1 illustrates in a simple way the basic principles of a retrieval that exploits the relation between the cloud radar observations and the optical depth information determined from MODIS radiances matched to the radar which is made possible by the formation flying aspects of the mission. The CloudSat algorithms based on this concept, however, are implemented observing the following requirements:

- Have a sound physical basis. Although this basis is illustrated in Fig. 1, the relationships expressed in that figure are formerly stated as

$$y=f(x,b)+\varepsilon_y \tag{1}$$

where y is the measurement (radar reflectivity and radiance data converted to optical depth), $f(x,b)$ is the forward function (i.e. a model) relating the desired information x to y involving parameters b provided from some other data base. Equation (1) is 'inverted' by an estimation procedure (e.g. Austin and Stephens, 2000) to provide the necessary information about clouds.

- Provide an associated error analyses – the estimation procedure requires specification of the errors associated with any *a priori* data base x_a, specification of errors arising from the forward model f and related parameters b, and specification of measurement error ε_y. The diagnosis of retrieval error that is

an output of the retrieval is also of elementary importance to application of the data in assimilation studies.

- Offer diagnostic measures of retrieval quality including some idea of the information content of the relevant measurements in relation to the given product

An example of this retrieval applied to synthetic radar observations derived from cloud profiles with varying amounts of precipitation is provided in Fig.2a-d and taken from the work of L'Ecuyer and Stephens (2001). The retrievals were performed using 94 GHz radar profiles simulated using the GPROF data base as input (Ohlsen et al., 1996) and do not attempt to add additional information to constrain attenuation by the precipitation. Shown in Figs. 2a and b are the rainfall retrievals at 2.5km and at the surface compared to the actual rainfall information of the GPROF database. Respective measures of the information content of the radar measurement are provided in Figs. 2c and d. The examples demonstrate a capability for retrieving surface precipitation for rain-rates below 3mmhr^{-1} without any significant ambiguity introduced by attenuation by rain. This capability is extended to even higher rain rates at levels above the surface. The capability portrayed in Figs. 2a and b is further emphasized in Figs. 2c and d. Shown are values of the A parameter (Marks and Rodgers, 1993) indicating the extent that the retrieved information is derived from the measurements. To guide in the interpretation, values of A that approaches unity imply retrievals that increasingly depend on the measurement whereas values approaching zero indicate retrievals that increasingly rely on extraneous information. Research is continuing on possible ways of dealing with the ambiguity associated attenuation thereby extending the validity of the retrievals to higher rain-rates (L'Ecuyer and Stephens, 2001).

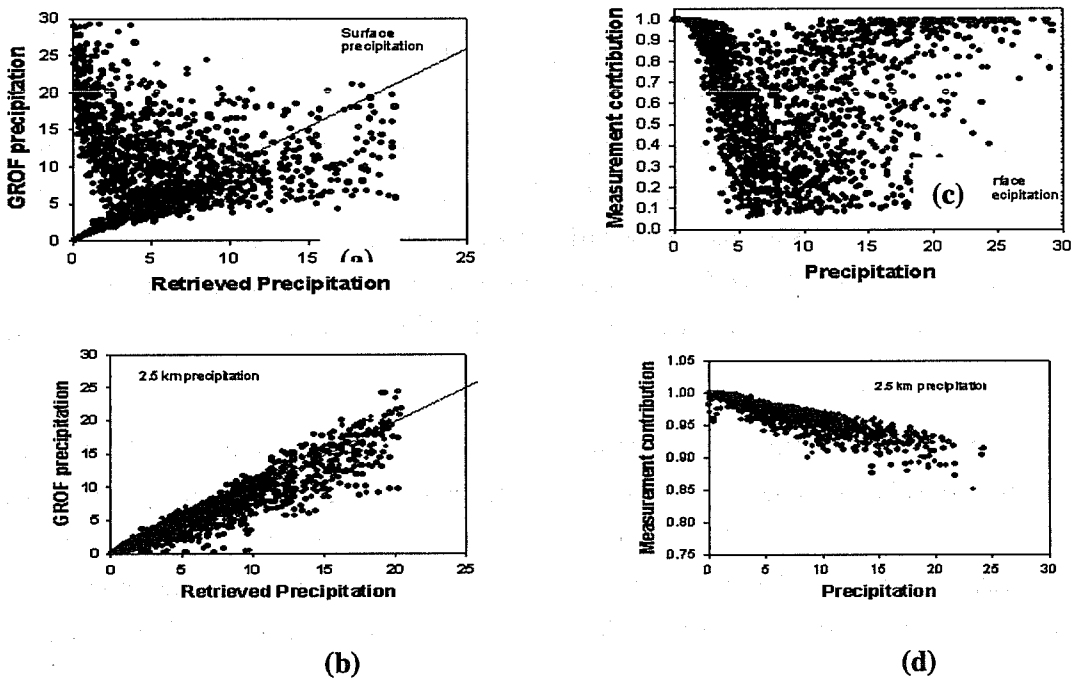

Fig. 2a-d. Synthetic retrievals of precipitation based on 94 GHz radar reflectivity profiles simulated from the GPROF data base compared to actual precipitation at the surface and at 2.5 km (a,b) and the corresponding a priori parameter derived for each retrieval (c,d). Precipitation is in mmhr^{-1}.

3.2 *Error and Evaluation*

Not only is the development of retrieval methods aimed at producing new information, an activity that will continue in the coming years, but also evaluation of both the standard and experimental products is to be an important focus of activity. The purpose of this evaluation activity is to quantify the error characteristics of the retrieval approach. There are two types of errors, random and bias errors and there are three basic sources (e.g. Austin et al., 2001):

- *Model error*– errors associated with the model of observation (radiative transfer model, radar equation, etc), and uncertainties in those parameters not retrieved but which establish the forward model. This error is typically a substantial part of the error budget of cloud & precipitation information extracted from retrieval algorithms.

- *Measurement error* – measurement error relates to instrument performance, calibration, noise, etc. For cloud and precipitation, measurement error (brightness temperatures, solar & IR radiances, radar reflectivities) is typically the smallest source of retrieval uncertainty.

- *Data base error* – uncertainties in *a priori* data-bases used to constrain non-unique solutions (e.g. multiple rain rates for a given brightness temperature) are an additional source of retrieval error that is often a significant but generally overlooked.

Four activities represent the approach to evaluate these errors:

- *Sensor Calibration*: Radar calibration includes a routine and detailed system calibration both in flight and prior to launch, vicarious calibration associated with surface returns from the ocean, and direct measurement comparisons with independently calibrated airborne radar.

- *Ground Truth* – this provides confirmation of the total error estimate which is also the output of the retrieval. It requires independent data obtained from (say) cloud physics probes that offer a more direct (and generally more accurate) measure of the relevant quantities being evaluated. There is generally no absolute ground truth and it is difficult to match these direct measurements with those derived from remote sensors due to the differences in sample of the two types of data. Quantifying total error is often times elusive for this reason but ground truth exercises remain important especially since these activities are the only way to estimate the difficult-to-determine systematic errors in the retrievals.

- *Error Modelling*: this activity attempts to quantify individual error components with the focus on those that are typically the largest source of retrieval error. For clouds and precipitation, these sources of error are typically attached to f, and b (the data base). The approach can vary and do not necessarily require equivalent radar observations as used by the retrieval algorithm. For CloudSat, these analyses make use of a variety of data sources including currently archived cloud physics data (e.g. Austin et al., 2000).

- *Consistency analyses*: for this activity, the retrieved information is compared to other information that is in one way or other correlated with the cloud information in question. This other information may typically come from a retrieval using independent data from other sensors (MODIS and AMSR radiances are specific examples). These kinds of comparisons provide a simple and expedient way of checking large volumes of data to identify possible failures in the retrieval while on orbit.

Figure 3 highlights this evaluation approach providing an example of 'ground-truth' comparisons of cloud radar LWC retrievals matched to *in situ* aircraft measurements and an example of consistency of information in the form of a comparison of cloud radar based LWP information matched and compared to LWP derived from an up-looking microwave radiometer (Austin et al., 2001). The rms deviation of both comparisons is about 30%. The actual total error is likely to be smaller than this since no attempt has been made in these comparisons to remove sampling errors that arise from the basic differences in sampling volume of the sensors used to produce the respective data.

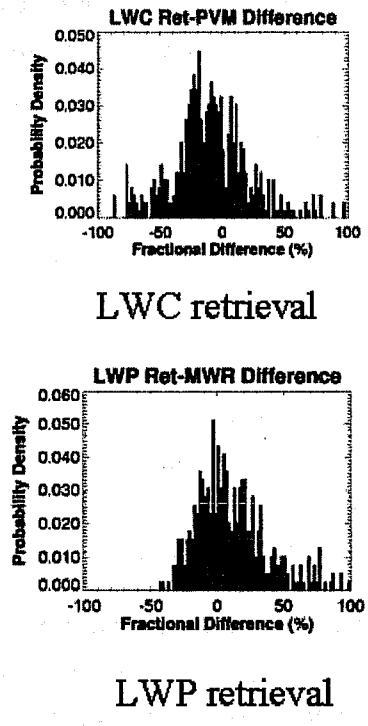

Fig. 3 An example of a form of ground truth comparison expressed in terms of a difference pdf derived from retrieved liquid water content using the CloudSat algorithm applied to airborne data (Austin et al, 2001) and in situ measurements of LWC (upper panel). A similar comparison between retrieved LWP and that derived from microwave radiometer measurements (lower panel).

4 Thoughts on Assimilation of Cloud Data

The challenges of assimilating cloud and precipitation data can conveniently be introduced by reference to the general cost function

$$J(x) = (x - x^b)^T B^{-1} (x - x^b) + (H(x) - y)^T (O + F)^{-1} (H(x) - y) \quad (2)$$

where x is the relevant parameter of interest, x^b is the background estimate of this parameter, H(x) is the forward model that maps x to a measurement y. B,O and F are respective error covariances associated with the forecast model, the observation y and the forward model H respectively. The assimilation problem seeks an x at the minimum of J(x). Various approaches may be adopted to seek this minimum and those in practice today in operational mode typically linearize the models implied in (1) in some way.

A number of issues emerge when considering (1) above within the context of cloud and precipitation assimilation:

What are the relevant measurements y? At what point do these measurements get introduced in the form of retrieved parameters versus in the form of an actual measurement? Limited cloud and precipitation assimilation studies that exist tend to treat y as a retrieved parameter, e.g. precipitation rather than an actual instrument observation. Answers to these questions dictate answers to the following:

What is x? These are parameters derived from the forecast model. At what point do we decide to treat x as conventional parameters (temperature, humidity, wind fields) or as an extended vector including additional non-conventional cloud parameters? This decision is crucial as it establishes the nature of the error covariances required to evaluate J(x).

What is H(x)? The answer to this depends on what is considered to be y and subsequently H(x). For one approach, H(x) includes the model physics that connects conventional parameters x (temperature and humidity for instance) to the cloud parameters y (precipitation) introduced via a retrieval. That is H(x) represents the cloud model component of the forecast model.

What do O,F and B represent? It is crucial that we be clear on the interpretation of these errors and furthermore have a strategy to estimate their magnitudes. O represents the error in y and depending on the choice of y this could either be the measurement error per se or the retrieval error. F then could be the error of the forward model such that F+O is the total retrieval error or F could be the error attached to the cloud parameterization of the forecast model. B is the background error of the model as it related to x. Therefore depending on the definition of x, B could represent the model error attached to conventional fields (for which more is known) or alternatively the model error that includes errors in the cloud parameterization scheme (for which little is known).

While answers to these questions remain an open issues of ongoing research, the above discussion points the importance of knowledge of measurement and retrieval error and the associated error of the model. The latter unavoidably requires specification of error associated with the cloud parameterization scheme whether this error is placed in B or resides in F.

5 Assimilation Cloud Radar Data in a simple model of cirrus

The following describes a series of numerical experiments in which synthetic cloud radar data are assimilated into a simple model of cirrus clouds. This work is described in more detail in Benedetti et al. (2001). The purpose of the experiments is to provide a format to consider some of the issues raised above and to expose other issues relevant to the assimilation of cloud measurements and specifically measurements provided by a 94 GHz cloud profiling radar.

5.1 A 2-D Lagrangian model of cirrus

The cirrus microphysical model described here is based on the work of Mitchell (1994, 1991, 1988), Passarelli (1978) and Drake (1972). Mitchell (1994)'s formulation has been extended to obtain two coupled prognostic equations to predict the time and vertical evolution of two parameters of a gamma size distribution of fixed width, the characteristic diameter D_n and the total number concentration of ice crystals N_t. These parameters are related through an assumed form of the particle size distribution

$$n(D) = N_t \frac{1}{\Gamma(\nu)} \left(\frac{D}{D_n} \right)^{\nu-1} \frac{1}{D_n} e^{-D/D_n}$$

from which the following parameters

$$\begin{aligned} m &= \alpha D_n^{\beta} \\ v &= a D_n^{b} \\ Z &= f(N_t, D_n) \end{aligned} \tag{3}$$

can be derived where respectively m represents the mass content, v the fall velocity and Z is the radar reflectivity. The quantities a, b α and β are pre-chosen coefficients taken from Mitchell (1988) and assumed constant for simplicity.

Two coupled equations follow from a Lagrangian time-dependent model equation that predicts the evolution of ice particle size spectra in cirrus clouds in terms of the growth by vapor diffusion and aggregation (break--up processes are not included).

This equation in flux form is:

$$\frac{\partial n_m}{\partial t} + \nabla \bullet n_m u = -P - VD + AG - AL \tag{4}$$

where n_m is the mass distribution, P is the loss by precipitation, VD the loss by vapor deposition from one mass bin to another, AG and AL represent gains and losses of ice mass by the process of aggregation. Because the ice-water content and reflectivity are directly proportional to the first and second moments of the mass distribution, it is possible to convert (4) into individual prognostic equations for each of these moments leading to a pair of differential equations, which may be integrated forward in time. Details of the

form of the source-sink terms in (4) expressed in terms of m and Z can be found in Benedetti et al., (2000). Prognostic equations for N_t and D_n then follow from the relations introduced above for m and Z.

The model is initialized with arbitrary profiles of diameter and number concentration. The initialization of the thermodynamical variables - temperature, specific humidity as well as the dynamical variables - vertical wind are taken from an ECMWF forecast for a case observed during an aircraft experiment off the island of Kuaui. The model is then integrated forward in time yielding new profiles of ice water content, Z, N_t and D_n. Figure 4 provides an example of the realism of the simulation of radar reflectivity predicted by this simple model compared to reflectivity derived from the grid-point ice water content of ECMWF forecast model. The forecast profiles have been matched in space and time to aircraft measurements as reported previously by Stephens et al. (2000). The profile of reflectivity derived from cloud resolving model ice water contents is also presented. All models reproduce credibly the features of the observation in varying degrees of detail.

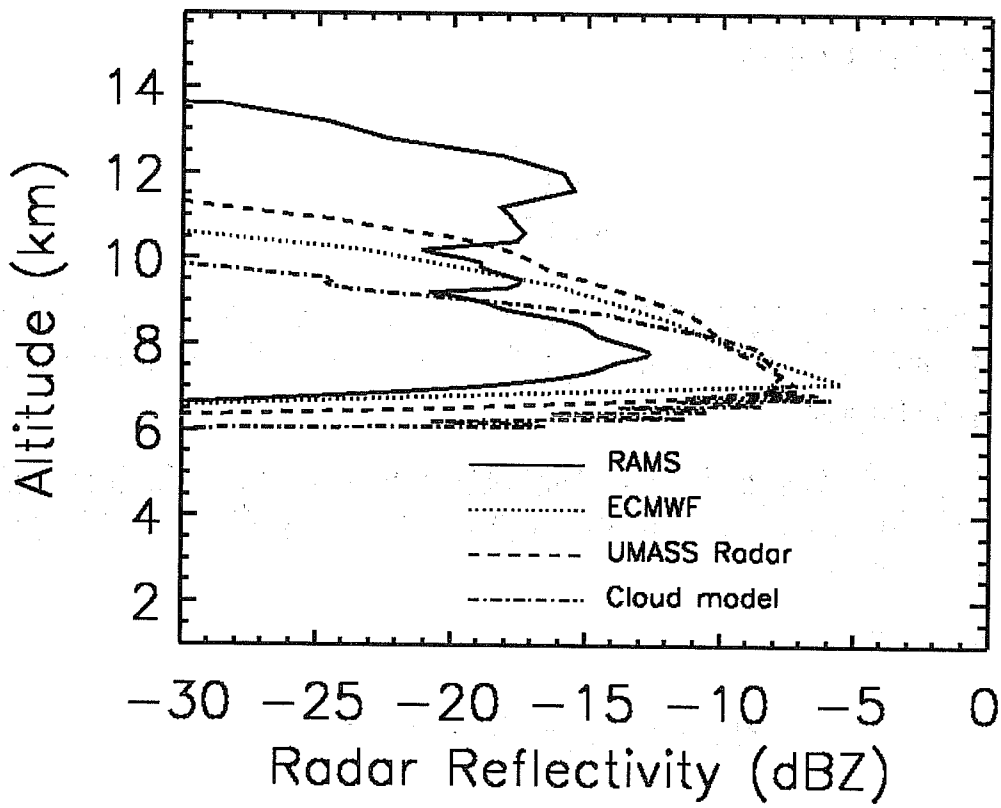

Fig. 4 Comparison of profiles of cloud reflectivity derived from three very different models of cirrus clouds compared to actual aircraft radar observations of cirrus. The ECMWF model profile is derive from forecast model fields for a particular cirrus case studied off Kuaui. The cloud resolving model and the Lagrangian cloud model were initialized using the background state variables obtained from the forecast. The profile labeled as cloud model represents the results of integrating the Lagrangian model forward in time for 30 minutes.

5.2 *Variational technique and the adjoint of the cirrus model*

The approach developed to assimilate radar reflectivity observations into the simple model described above seeks to estimate that set of cloud parameters, in this case profiles of N_t and D_n, that minimize the cost function

$$J(x) = \frac{1}{2}\int \left[(x - x^b)^T B^{-1}(x - x^b) + (H(x) - y)^T (O + F)^{-1}(H(x) - y)\right] \delta(t - t_{obs})\, dt \qquad (5)$$

where H(x) maps the state variables x=(N_t, D_n) into the observational space y=Z of radar reflectivities and errors in this mapping are assumed to arise only from the radar forward model and from the observations. The dynamical (cloud) model error is assumed to be zero. The first term of the right hand side of (5) requires a specification of the background error covariance (B^{-1}) and some definition of the background state x_b taken to be the initial profiles of N_t and D_n (both chosen arbitrarily).

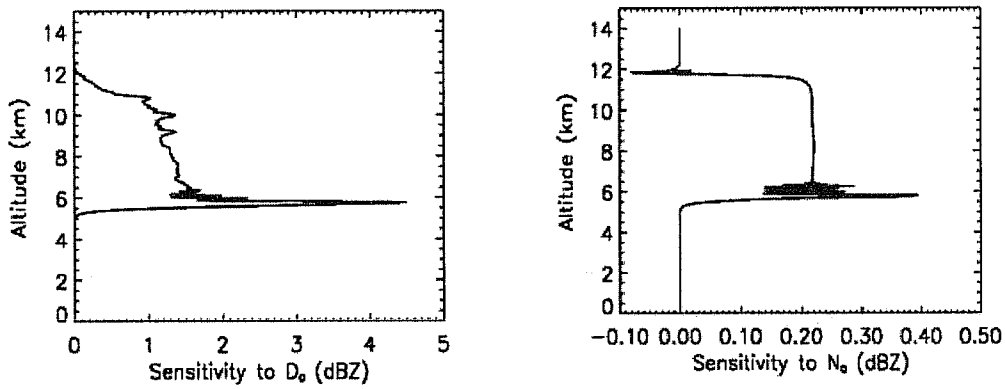

Fig. 5 Profiles of the sensitivity of Z due to variations of both N_t (right) and D_n (left) as derived from the adjoint of the cloud model.

A set of observations is specified at discrete time periods t_{obs} and details of the optimization procedure adopted to minimize J(x) are described in Benedetti et al. (2001).

The procedure requires the adjoint of the cloud model which was derived using the tangent linear and adjoint compiler (TAMC) developed by Giering (1999). This adjoint provides a way of quantitatively assessing the sensitivity of the measurement (Z) to the state variables N_t and D_n. Examples of the sensitivities derive from the model adjoint are provided in both Fig. 5 and Table 2. Figure 5 presents profiles of the sensitivity of Z due to variations of both N_t and D_n. The results demonstrate the expected result that the sensitivity to D_n is six-fold larger than the sensitivity to N_t. Table 2 summarizes the sensitivity of optical depth (another potential form of observation) to variations in various cloud parameters listed.

Parameter	Sensitivity
N_t	0.0126
D_n	0.0242
Vapor diffusion coeff.	0.001
Fall speed parameter a	-6.5e-5
Fall speed parameter b	-0.0012

Table 2 Sensitivity of optical depth to a 5% change of stated parameter

The largest sensitivity is that due to variations of N_t and D_n where again as expected the sensitivity to D_n is twice that due to N_t. The sensitivities of Z and optical depth to variations of N_t and D_n differ from one another re-asserting the assumptions of the CloudSat retrieval that each type of measurement contains sufficiently different information about these parameters permitting their retrieval.

5.3 Assimilation Results

Synthetic radar measurements were created from an assumed initial profile of N_t and D_n. This resulted in a single Z profile. Similarly synthetic optical depths were also computed using an appropriate forward model for this information. The model uses perturbed initial profiles of N_t and D_n and the optimization is performed with the synthetic observations assimilated at discrete assimilation time intervals (i.e. the same Z profile and optical depths were assimilated every 5 minutes of model integration). The perturbed initial condition was defined as a given fixed percentage of the "true" initial condition. It was found that for perturbations up to 50% of the true initial condition convergence was obtained and the true initial profiles of characteristic diameter and number concentration were perfectly recovered (Fig. 6). The number of iterations required for convergence varied according to the magnitude of the perturbations (i.e the proximity of the initial model profiles to truth). Experiments were also performed in which uniform random noise was added to a 15% perturbed initial condition, and the optimization perfectly succeeded, yielding the true initial condition as output.

Convergence could not be obtained when the position of the cloud layer in the perturbed case was misplaced with respect to the true initial condition (and hence the observations), even for relatively small percentage perturbations in N_t and D_n and small misplacements.

Figure 7 show results for a 50% perturbation in initial condition, with the cloud also misplaced with respect to truth by 1 km. The results of the optimization are given in Fig. 7c. No convergence was achieved and the initial profile could not be recovered.

The example of Fig. 7 represents a very limiting factor for the assimilation of real measurements, since it seems that the model is not able to adjust the cloud variables in region where no cloud is present to begin with. This also indicates that it might be better to assimilate other thermodynamic variables, such as relative or specific humidity and temperature, rather than cloud variables.

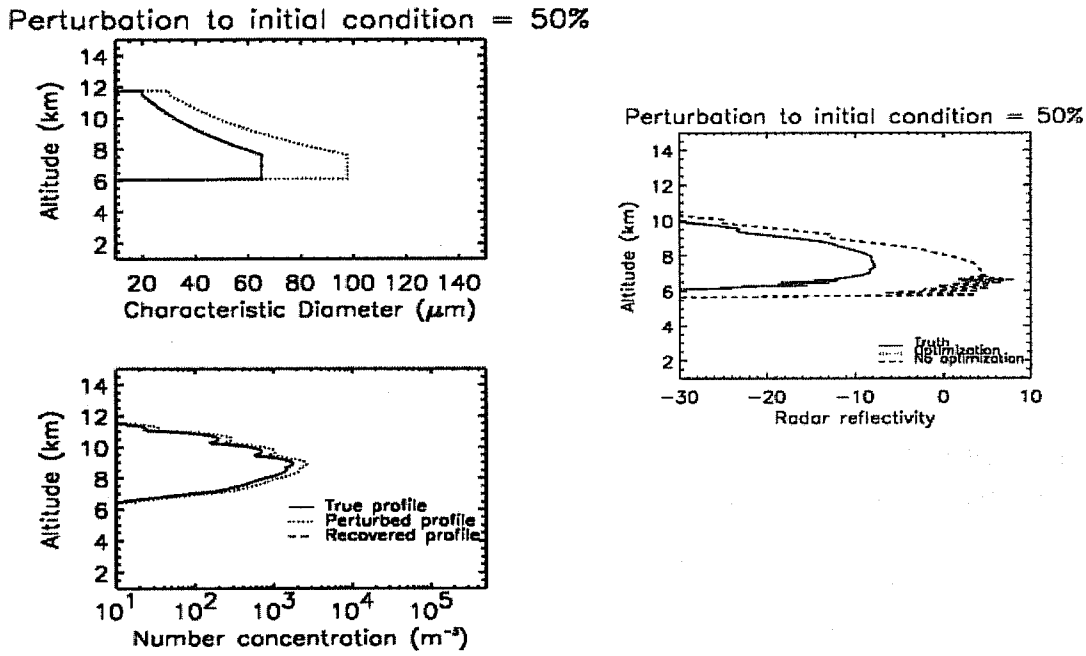

Fig.6 (left top and bottom) True initial conditions for D_n and N_t (solid lines) and the perturbation profiles (dotted lines) (right) Synthetic measurements and the recovered reflectivity profile at final time after optimization is performed. The short--dashed line represent the reflectivity profile for perturbed initial condition. The recovered profile after assimilation (dotted) falls precisely on the measured profile (solid).

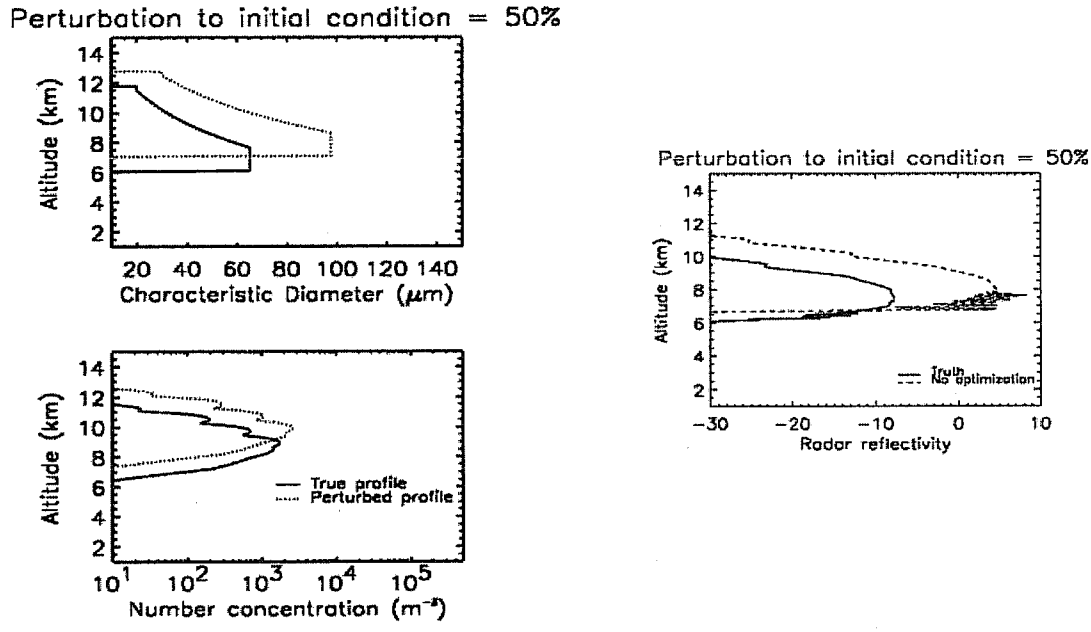

Fig. 7 as in Fig. 6 Synthetic measurements and the initial perturbed profile. Unlike in Fig. 6, no final solution was obtained.

In general the results indicate that assimilation of cloud radar data into a cloud model is in principle feasible and meaningful, but as with other studies, real difficulty is encountered when the model and observations are not close to each other with respect to actual placement of the cloud. Overcoming this general problem is challenging and solution to it will involve a closer look at the particular variables that need to be included in the adjustment in the variational optimization.

6 Concluding Comments

CloudSat is a satellite experiment designed to provide, as directly as possible, information relevant for assessing the way cloud processes are parameterized in global weather prediction and climate models. In this way, CloudSat will provide a means for the critical evaluation of model prediction of clouds. This information is to be extracted from vertical profiles of radar reflectivity obtained with the CloudSat 94 GHz nadir pointing radar. The information includes: profiles of cloud occurrence determined from radar reflectivity thresholds from which vertical structure information (cloud top, base, thickness, overlap) is derived. Next are the associated profiles of cloud water and ice contents derived from the profiles of reflectivity (and other information such as optical depth as provided by sensors flown on other satellites flown in formation with CloudSat). This information, together with a cloud classification derived from the radar and imaging data, constitutes the suite of standard data products to be processed by the CloudSat data processing center located at CIRA in Colorado. These standard products will be made available to the open community shortly after launch (3-4 months after observation). In addition to the standard products, a suite of experimental products is being developed and will also become available to the community by consulting with relevant science team members responsible for that product. A key experimental data product is the precipitation liquid (and perhaps solid) water content and together with the cloud information, forms a powerful and unique combination of data to test cloud parameterization.

CloudSat as described above is an experimental mission providing the above-mentioned data for a proposed two-year period and then only along a narrow swath defined by the non-scanning, nadir pointing radar producing a footprint slightly larger than 1 km. By nature of these data do not lend themselves to assimilation in global, operational models. However CloudSat can be expected to progress the problem of assimilation in a number of important ways:

- CloudSat data provides the most unambiguous and quantitative way of verifying the performance of prediction models. This evaluation will lead to improvements of parameterization methods on the one hand and better understanding of model error on the other hand.

- CloudSat data can be expected to stimulate progress on the problem of cloud data assimilation. The simple example presented in this paper represents a preliminary step in this direction.

There remain a number of formidable steps confronting progress in the assimilation of cloud and precipitation information. The involvement of CloudSat in research on this topic is important for a variety of reasons. Progress on assimilation of cloud radar data, even in the more experimental setting of the research described in this paper, provides a quantitative way of assessing the impact of these observations

on models and related model improvements perhaps leading to a clearer vision for future clouds and precipitation observing systems.

7 Acknowledgements

This work has bee supported by NASA research Grants NAG#5-6637 and NAS5-99237.

8 References

Austin, R. and G. Stephens, 2001; Retrieval of stratus cloud microphysical parameters using millimetric radar and visible optical depth in preparation for CloudSat: I Algorithm basis, submitted to *J. Geophys. Res.*

Austin, R., G. Stephens, S. Miller, S. Sekelsky, F. Li and Q. Min, 2001: Retrieval of stratus cloud microphysical parameters using millimetric radar and visible optical depth in preparation for CloudSat: II Algorithm validation, submitted to J. Geophys. Res.

Benedetti, A, G. Stephens and T. Vukicevic, 2001; On the Assimilation of cloud radar reflectivities in a cirrus model using a 2D-Var approach, submitted to Quart. J. Roy. Met. Soc.

Drake, R.L., 1972; The scalar transport equation of coalescence theory: moments and kernels, J. Atmos. Sci., 29, 537-547.

Giering, R., 1999; Tangent linear and Adjoint Model compiler, User's manual 1.4, *htpp://puddle.mit.edu/~ralf/tamc*

L'Ecuyer, T. and G. Stephens, 2001; An estimation-based precipitation retrieval algorithm for attenuating radars, submitted to *J. Appl. Met.*

Marks, C. and C. Rodgers, 1993; A retrieval method for atmospheric composition from limb emission measurements, *J. Geophys. Res.*, **98**, 14939-14953.

Mitchell, D., 1991; Evolution of snow-size spectra in cyclonic storms. Part I: snow growth by vapor deposition and aggregation, *J. Atmos. Sci.*, **45**, 3431-3451.

Mitchell, D., 1991; Evolution of snow-size spectra in cyclonic storms. Part II: deviations from the exponential form, *J. Atmos. Sci.*, **48**, 1885-1899.

Mitchell, D., 1994; A model predicting the evolution of ice spectra and radiative properties of cirrus clouds. Part I: Microphysics, *J. Atmos. Sci.*, **51**, 797-816.

Olsen, W., C Kummerow, G. Heymsfield, and L. Giglio, 1996; A method for combined passive-active microwave retrievals of cloud and precipitation profiles, *J. Appl. Met.*, **35**, 1763-1789.

Passarelli, R.E., 1978; Theoretical and observational study of snow-size spectra and snowflake aggregation efficiencies, *J. Atmos. Sci.*, **35**, 882-889.

Stephens, G., D. Vane, and the CloudSat science team; 2000; CloudSat: a new dimension in the observation of clouds from space, submitted to *Bull. Amer. Met. Soc.*